Nanostructured interfaces between photosynthetic bacterial Reaction Center and Silicon electrodes

Marco Lo Presti[1], Danilo Vona[1], Gabriella Leone[1,2], Giorgio Rizzo[1], Roberta Ragni[1], Stefania R. Cicco[3], Francesco Milano[4], Fabio Palumbo[5], Massimo Trotta[6]*, Gianluca M. Farinola[1]*

Corresponding Authors: massimo.trotta@cnr.it; gianlucamaria.farinola@uniba.it

[1]*Dipartimento di Chimica, Università degli Studi di Bari Aldo Moro, Via Orabona 4 70126, Bari Italy*

[2]*Centro di nanoscienza e tecnologia IIT-CNST, via Pascoli 70 20133, Milan Italy*

[3]*Dipartimento di Chimica, Consiglio Nazionale delle Ricerche-Istituto di Chimica dei Composti OrganoMetallici (CNR-ICCOM), Via Orabona 4 70126, Bari, Italy*

[4]*CNR-ISPA, Institute of Sciences of Food Production, Lecce Unit, Via Prov.le Monteroni, 73100 Lecce, Italy*

[5]*Istituto per Metodologie Organiche e Plasmi (IMIP)-CNR, Via Amendola 122/d-o 70126, Bari, Italy*

[6]*Istituto per i processi Chimico-FIsici (IPCF), CNR, Via Orabona 4, 70126, Bari, Italy*

ABSTRACT:

Optimizing interfaces between photosynthetic natural photoconverters, like photosynthetic bacterial Reaction Centers (RCs) and electrode surfaces represents a challenge in the progress of bio-optoelectronic devices. The features of the surfaces may result detrimental for the tertiary and quaternary structures of the RC, even resulting in the denaturation of the enzyme. Functional surfaces possessing both confinement capability and conductive features able to preserve the conformation of the biomolecule and its bioelectronic behaviours are highly needed. In this work, the RC is adsorbed on diatomaceous silica and plasma treated hydrophobic silicon based materials. Both the materials are demonstrated to be able to

preserve and enhance the RC photoconverting activity. In particular, we evaluate the functioning of isolated bacterial RC interacting with flat pSi electrode through two nanotextured interfaces designed to address the RC: a thin conductive silicon film nanotextured in pillars via plasma treatment, and a cast film of nanostructured dielectric biosilica obtained from diatomaceous earth. The characterization of these interfaces, together with the RC photocurrent production measurements, pave the way to new generation RC based bio-devices for photocurrent investigation.

INTRODUCTION:

Bionanocomposites, among other biohybrid systems, exhibit features suitable for several applications including biosensors, integrated (opto)electronic switches, photoconverters and systems for molecular imaging. [1-3] Biohybrid devices can be based on different classes of materials, including small molecules for organic electronics, [4-6] organic polyconjugated semiconductors [7-10] or biological and biomimetic components as active materials, ranging from biopolymers [11-13] up to living cells. [14-15]

To this purpose, the use of photosynthetic enzymes that proficiently perform transduction of light into charge separated states represent an appealing route to sustainable energy sources. The bacterial Reaction Center (RC) is a highly efficient photoconverter, [16] a transmembrane photoenzyme that converts photons absorbed by photoactive antennas into electron:hole pairs. The production of functional nanomaterials based on this natural photoconverter is an attractive possibility for bioelectronic applications. [17] RC-organic biohybrid systems of poly-conjugated antennas directly bonded to the RC have been proposed for increasing the light harvesting capability of RC. [18-20] It has been also demonstrated that RC embedded in soft structures, like lipid vesicles, [21] liposomes [22] or polymersomes, can maintain its activity without being denatured. [23]

Interfaces between photosynthetic RC and inorganic electrode surface of optoelectronic films, which are commonly made of inorganic materials devices, still represent an issue. The possibility to integrate RCs from various photosynthetic organisms into silicon, after silica coated electrodes, still presenting the structure and function has been demonstrated. RCs from different organisms have been integrated in silicon [24] and silica confinement systems, [25] preserving their structures and functions. Synthetic mesoporous silica has been also used. [26] Similarly, Si-based material consisting of conductive P-doped silicon has been successfully proposed to this aim, due to its easily tunable pore dimensions, large surface area, [27-28] integration in photonic structures [29] and its natural biodegradability. Recently, RC from *Rhodobacter (R.)* has been conjugated to porous silicon microcavities through silane-glutaraldehyde chemistry or *via* noncovalent peptide cross-linking: the resulting complex possesses enhanced ability to generate charge separated states and to induce redox changes on cytochrome c, indicating that the RC main sites were still accessible to external electron carriers. [30]

The activity of RC on two different electrode surfaces able to perform a nanostructured confinement of the photoconverter was tested: the hydrophobicity of the silicon material and the nanostructure of the electrode surfaces promote the adsorption of the enzyme. In particular, we measured the photocurrent of RC adsorbed on different substrates: flat (pSi), hydrophobic plasma textured silicon (npSi:pSi) and natural mesoporous biosilica from microalgae casted on flat silicon (ntSilica:pSi). Mesoporous biosilica from algal biomass has been already used for confining drugs or biomolecules.

[31-32] The two surfaces bid the possibility to exploit RC systems as light-activated element between the silica electrode and redox partners in the bulk solution.

RESULTS AND DISCUSSION:

Preparation of substrates and SEM characterization

For the preparation of ntSilica:pSi samples, diatomaceous earth (DE) was purified and casted on pSi, as reported in Materials and Methods Section. DE was casted once or three times in order to produce dielectric:conductive samples with different thickness (referred as DE1 and DE3, respectively). The casting process was followed by thermal annealing to fix DE on Si surfaces.

P-doped crystalline silicon wafer was textured using CF_4 plasma for producing nanotextured surfaces (see Materials and Methods Section). Two different pillars morphologies (Rodo1 and Rodo2) were obtained under two different treatment times of 10 and 20 minutes.

Diatomaceous earth (DE) dielectric nanostructured layers on the conductive pSi have been examined by SEM, as reported in Figure 1. In the DE1 (Figure 1a) and DE3 (Figure 1b) of purified DE on pSi, integer or parts of frustules from pennate and centric species are evident together with silica rods debris, clasps, girdles. The inset focus shows nanotextures of the sub-structures from DE biosilica elements. This naturally nanotextured silica creates a confining and dielectric layer onto conductive pSi, since most nanofeatures can be exploited to physically entrap and protect RCs. SEM images of Rodo1 and Rodo2 npSi:pSi samples, obtained *via* CF_4 plasma, are reported in figure 1c and 1d, respectively. The more treated plasma sample (Rodo2) showed taller and wider pillars, compared to the less treated one (Rodo1). In particular, an average pillar height of 0.9 µm was obtained in the case of the 10' plasma treatment. Doubling the treatment time leads to an average height of 1.7 µm.
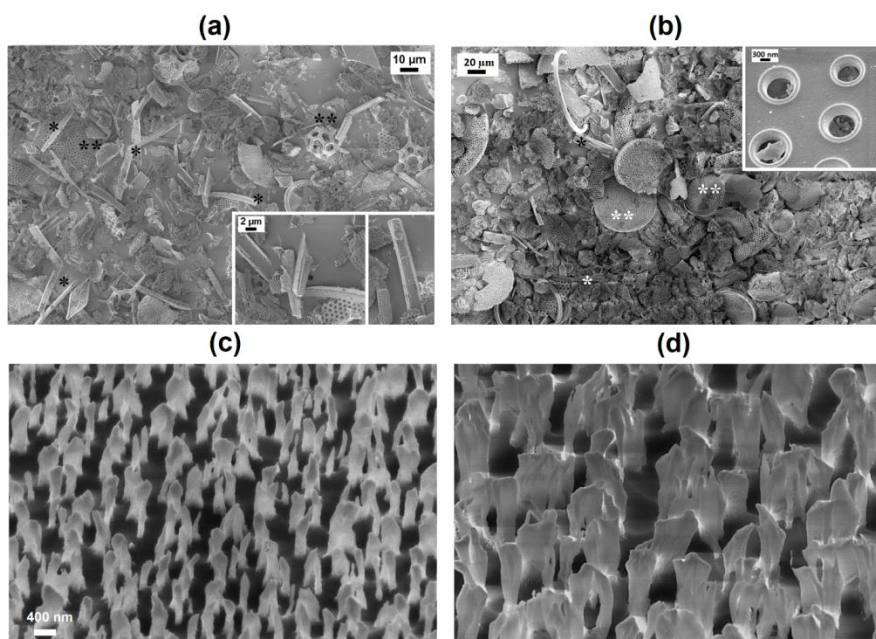
Figure 1. SEM images of 1 layer (a) and 3 layer (b) of purified DE on pSi after thermal annealing. Frustules from pennate (*) and centric (**) species are evident. Inset focus: nanotextures or sub-structures from DE biosilica elements. SEM images of Rodo1 (c) and Rodo2 (d) CF$_4$ plasma treated silicon at a tilt angle of 45° with 50Kx magnification.

Photocurrent measurements of RC in integrated systems

Flat pSi, npSi:pSi, and ntSilica:pSi were used as working electrodes (WE) in chronoamperometric measurements. A constant potential of -0.2 V was applied, as suggested by literature, [33] generating a cathodic current during illumination in all cases, indicating a light-induced reduction process at the WE. The flat pSi shows negligible photocurrent in the presence of the RC and redox mediators. This is likely associated with the lack of the RC confinement on the flat pSi that favours redox reaction occurrence only in solution.

The addition of the diatomaceous nanostructured natural silica layers on the conductive Si electrode (Figure 2) produces a bifunctional dielectric:conductive device (ntSilica:pSi) that generates photocurrents. This is likely due to the establishment of RC-electrode communication. Nevertheless, single layer nanostructured silica (DE1) shows higher photocurrent with respect to the 3 layered dielectric sample (DE3). This effect is likely due to a decreased electrode conductivity consequent to the increase of the silica layer thickness.

In the case of plasma treated electrodes Rodo1 and Rodo2, the experiments display (Figure 2) higher photocurrents than DE1 and DE3. Electrode performance increases presumably because of the higher hydrophobicity of Rodo# samples, which stabilize the hydrophobic domains of the RC. Furthermore, a higher surface availability of these textured electrodes improves the RC-electrode interactions. Notably, Rodo2 exhibits lower photocurrent than Rodo1 conceivably associated with larger and less entrapping pillars coverage of the surface. The current densities on the immersed

electrode surface (45 mm^2) were respectively 0.17 and 0.04 ($\mu A/cm^2$) for DE1 and DE2, 0.80 and 0.71 ($\mu A/cm^2$) for Rodo1 and Rodo2.
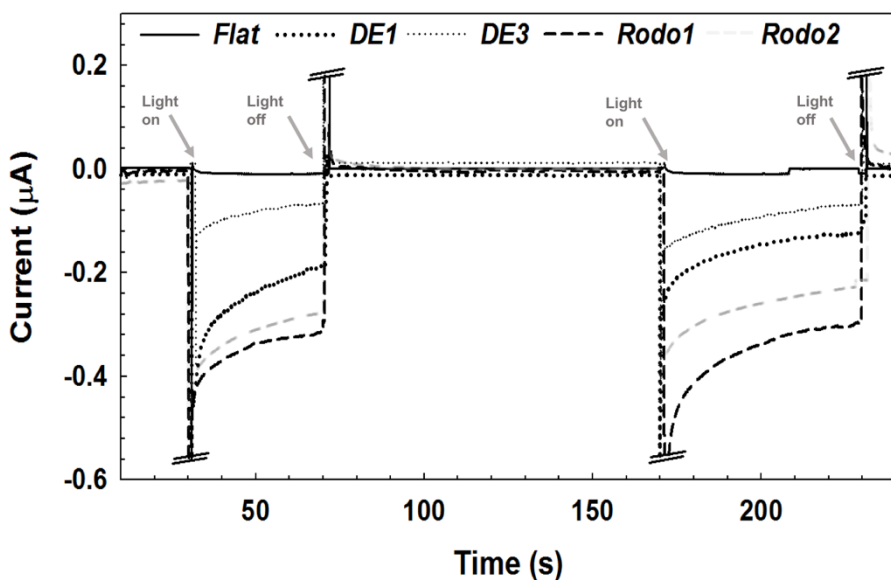
Figure 2. Chronoamperometric profiles in P$_{100}$ pH 7.0 with redox mediators FeCN:MeOH 200μM and dQ 200μM, and RC 3μM, applying a potential of -0.2V, and using different substrates.

MATERIALS AND METHODS:

Surface Texturing of P-doped silicon

P-doped crystalline silicon slabs were plasma treated as reported in literature, to produce nanotextured surfaces. [34] Two different texturing times under the CF$_4$ plasma (10 minutes and 20 minutes) were used to produce 2 morphologies, referred respectively as Rodo1 and Rodo2 structures.

Biosilica purification from DE and casting of biosilica nanostructures

Based on a literature protocol, [35] an activation process of Diatomaceous Earth (DE) was exploited for purifying silica matrix from oxides. This method is commonly used for extracting living diatom biosilica [36-37] for photonics, [38] nanoparticles [39-40] and tissue engineering [41-42] applications. After the treatment, casting of the DE suspension in water:acetone 1:1 v/v (DE 4 mg/mL) on pSi, followed by thermal annealing on heating plate at 350°C for 1 hour, were performed in order to produce 2 types of ntSilica:pSi surfaces (1 or 3 layered of DE on pSi, referred as DE1 and DE3).

Scanning electron microscopy (SEM)

Scanning Electron Microscopy (SEM) was carried out to analyse the morphologies of npSi:pSi (Rodo1 and Rodo2) and ntSi:pSi (DE1 and DE3) samples with a Zeiss Supra 40 equipped with a Gemini field emission gun. Analyses were carried out at an extraction voltage of 5 kV, at a working distance of 5mm and a tilt angle of 0° and 45°.

Bacterial Culture and RC purification

The carotenoidless strain R26 of the photosynthetic bacterium *R. sphaeroides* was grown under phototrophic conditions according to previously published procedures. [43-44] RC photoenzyme was extracted and purified using a literature protocol. [45-46]

Electrochemical measurements

Photoelectrochemical measurements were conducted at room temperature in a three-electrode cell, adapted to a plastic cuvette (1x1 cm^2 base and 1.5 cm height) by using an Autolab potentiostat PGSTAT 10. Saturated Ag/AgCl electrode was used as reference and a Pt wire was used as counter-electrode. The pSi wafer was the working electrode (WE) and 1 mL of phosphate 100 mM, Triton X-100 0.03% pH 7.0 (P_{100}) water solution was the support electrolyte. The electroactive WE area was 9x10 mm^2. Ferrocene methanol (FeCN:MeOH) 200 μM was set as the electron donor whilst decylubiquinone (dQ) 200 μM as the electron acceptor. When added in solution, the RC concentration was fixed to 3μM. A bias of -0.2 V (corresponding to the OCV of the cell in the dark) was applied between the reference and the working electrodes. For the photocurrent generation, the WE, with the nanostructure side facing towards the light source, was illuminated with a 2.6 W LED emitting at 865 nm, where the sole absorbing specie is the RC, with an irradiance of 25 mW/cm^2 and a photon flux of 1.1×10^{17} photons/s·cm^2. Cycles of 30s and 60s of dark relaxation were used in the experiments.

CONCLUSIONS:

Different nanostructured interfaces have been assembled to convey photosynthetic bacterial RC onto coated electrodes and to investigate the generation of photocurrents under illumination. Photocurrent generation in conductive plasma treated npSi:pSi and dielectric:conductive ntSilica:pSi, bearing layers of diatomaceous earth silica textures, shows that coated electrodes are able to confine and fix RC within their texture.

Highest photocurrents were observed using the plasma treated nanotextured pSi, which appears to better promote the RC-electrode interaction. This effect could be a combination of the RC confinement with the hydrophobicity of the ntSi:pSi electrodes that well fits with the hydrophobic nature of the photoenzyme.

AKNOWLEDGEMENTS:

References:

[1] M. Darder, P. Aranda, and E. Ruiz- Hitzky, *Adv. Mater.* **19**(10), 1309-1319 (2007).
[2] M. T. Giardi, and E. Pace, *TRENDS in Biotech.* **23**(5), 257-263 (2005).
[3] P. Ormos, L. Fábián, L. Oroszi, E. K. Wolff, J. J. Ramsden, and A. Dér, *Appl. Phys. Let.*, **80**(21), 4060-4062 (2002).
[4] F. Babudri, D. De palma, G. M. Farinola, R. Ragni, and F. Naso, *Synthesis*, **2008**(8), 1227-1232 (2008).
[5] F. Babudri, A. Cardone, C. T. Cioffi, G. M. Farinola, F. Naso, and R. Ragni, *Synthesis* **2006**(08), 1325-1332 (2006).
[6] A. Punzi, D. I. Coppi, S. Matera, M. A. Capozzi, A. Operamolla, R. Ragni, and G. M. Farinola, *Org. Lett.* **19**(18), 4754-4757 (2017).
[7] D. Pisignano, L. Persano, R. Cingolani, G. Gigli, F. Babudri, G. M. Farinola, and F. Naso, *Appl. Phys. Lett.* **84**(8), 1365 - 1367 (2004).
[8] A. Operamolla, R. Ragni, H. O. Omar, G. Iacobellis, A. Cardone, F. Babudri, and G. M. Farinola, *Curr. Org. Synth.* **9**(6), 764-778 (2012).
[9] R. Ancora, F. Babudri, G. M. Farinola, F. Naso, and R. Ragni, *Eur. J. Org. Chem.* **2002**(24), 4127-4130 (2002).
[10] R. Ragni, A. Punzi, F. Babudri, and G. M. Farinola, *Eur. J. Org. Chem.* **2018**(27-28), 3500– 3519 (2018).
[11] M. Ambrico, A. Cardone, T. Ligonzo, V. Augelli, P. F. Ambrico, S. Cicco, G. M. Farinola, M. Flannino, G. Perna, and V. Capozzi, *Org. El.* **11**(11), 1809-1814 (2010).
[12] M. Ambrico, P. F. Ambrico, A. Cardone, N. F. Della Vecchia, T. Ligonzo, S. R. Cicco, M. Mastropasqua Talamo, A. Napolitano, V. Augelli, G. M. Farinola, and M. D'Ischia, *J. Mater. Chem. C*, **1**(5), 1018-1028 (2013).
[13] M. Ambrico, F. P. Ambrico, A. Cardone, T. Ligonzo, S. R. Cicco, R. Di Mundo, V. Augelli, and G. M. Farinola, *Adv. Mater.* **23**(29), 3332–3336, (2011).
[14] A. Operamolla, R. Ragni, F. Milano, R. R. Tangorra, A. Antonucci, A. Agostiano, M. Trotta, and G. M. Farinola, *J. Mater. Chem. C*, **3**(25), 6471-6478 (2015).
[15] F. Milano, A. Punzi, R. Ragni, M. Trotta, and G. M. Farinola, *Adv. Funct. Mater.* **1805521**, 1-17 (2018).
[16] F. Mavelli, M. Trotta, F. Ciriaco, A. Agostiano, L. Giotta, F. Italiano, and F. Milano, *Eur. Biophys. J.* **43**(6-7), 301-315 (2014).
[17] G. M. Farinola, R. Ragni, F. Milano, S. La Gatta, R. R. Tangorra, M. M. Talamo, M. Lo Presti, A. Agostiano, S. R. Cicco, A. Operamolla, H. O. Omar, and M. Trotta, *Org. Sens. Bioel. IX*, 9944, 1-6 (2016).
[18] F. Milano, R. R. Tangorra, O. Hassan Omar, R. Ragni, A. Operamolla, A. Agostiano, G. M. Farinola, and M. Trotta, *Ang. Chem. Int. Ed.* **51**(44), 11019-11023 (2012).
[19] O. Hassan Omar, S. La Gatta, R. R. Tangorra, F. Milano, R. Ragni, A. Operamolla, R. Argazzi, C. Chiorboli, A. Agostiano, M. Trotta, and G. M. Farinola, *Bioconj. Chem.* **27**(7), 1614-1623 (2016).
[20] S. La Gatta, F. Milano, G. M. Farinola, A. Agostiano, M. Di Donato, A. Lapini, P. Foggi, M. Trotta, and R. Ragni, *Biochim. Biophys. Acta. Bioenerg.* **1860**(1), 350-359 (2019).
[21] E. Altamura, F. Milano, R. R. Tangorra, M. Trotta, O. Hassan Omar, P. Stanod, and F. Mavelli, *Proc. Natl. Acad. Sci. USA*, **114**(15), 3837-3842 (2017).
[22] F. Milano, F. Italiano, A. Agostiano, and M. Trotta, *Photosynth. Res.* **100**(2), 107-112 (2009).
[23] R. R. Tangorra, A. Operamolla, F. Milano, O. H. Omar, J. Henrard, R. Comparelli, F. Italiano, A. Agostiano, V. De Leo, R. Marotta, A. Falqui, G. M. Farinola, and M. Trotta, *Photochem. & Photobiol. Sci.* **14**(10), 1844-1852 (2015).
[24] V. M. Aroutiounian, K. S. Martirosyan, A. S. Hovhannisyan, and P. G. Soukiassian, *J. Contemp. Phys. (Armenian Academy of Sciences)*, **43**(2), 72-76 (2008).
[25] C. F. Meunier, J. C. Rooke, K. Hajdu, P. V. Cutsem, P. Cambier, A. Leonard, and B. L. Su, *Langmuir*, **26**(9), 6568−6575 (2010).
[26] T. Noji, C. Kamidaki, K. Kawakami, J. R. Shen, T. Kajino, Y. Fukushima, T. Sekitoh, and S. Itoh, *Langmuir*, **27**(2), 705-713 (2010).
[27] E. Estephan, M. B. Saab, V. Agarwal, F. J. Cuisinier, C. Larroque, and C. Gergely, *Adv. Funct. Mater.* **21**(11), 2003-2011 (2011).
[28] G. Palestino, R. Legros, V. Agarwal, E. Pérez, and C. Gergely, *Sens. Act. B. Chem.* **135**(1), 27-34 (2008).
[29] M. M. Orosco, C. Pacholski, G. M. Miskelly, and J. Sailor, *Adv. Mater.* **18**(11), 1393-1396 (2006).
[30] K. Hajdu, C. Gergely, M. Martin, T. Cloitre, L. Zimányi, K. Tenger, P. Khoroshyy, G. Palestino, V. Agarwal, K. Hernà Dì, Z. Nè Meth, and Z. Nagy, *Langmuir*, **28**(32), 11866-11873 (2012).
[31] R. Ragni, S. R. Cicco, D. Vona, and G. M. Farinola, *Adv. Mater.*, **30**(19), 1704289-1704312 (2018).
[32] R. Ragni, S. Cicco, D. Vona, G. Leone, and G. M. Farinola, *J. Mater. Res.* **32**(2), 279-291(2017).
[33] G. LeBlanc, G. Chen, E. A. Gizzie, G. K. Jennings, and D. E. Cliffel, *Adv. Mater.* **24**(44) 5959-5962 (2012).

[34] M. Ambrico, P. Ambrico, A. Minafra, A. De Stradis, D. Vona, S. R. Cicco, F. Palumbo, P. Favia, and T. Ligonzo, *Sensors* **16**(11), 1946-1959 (2016).
[35] D. Vona, G. Leone, R. Ragni, F. Palumbo, A. Evidente, M. Vurro, G. M. Farinola, and S.R. Cicco, *MRS Adv.* **1**(57), 3825-3830 (2016).
[36] G. Leone, D. Vona, E. De Giglio, M. A. Bonifacio, S. Cometa, S. Fiore, F. Palumbo, R. Ragni, G. M. Farinola, and S. R. Cicco, *Data in Brief*, **24**, 103831-103840 (2019).
[37] D. Vona, L. Urbano, M. A. Bonifacio, E. De Giglio, S. Cometa, M. Mattioli-Belmonte, F. Palumbo, R. Ragni, S. R. Cicco, and G. M. Farinola, *Data in brief*, **8**, 312-319 (2016).
[38] R. Ragni, F. Scotognella, D. Vona, L. Moretti, E. Altamura, G. Ceccone, D. Mehn, S. R. Cicco, F. Palumbo, G. Lanzani, and G. M. Farinola, *Adv. Funct. Mater.* **28**(24), 1706214-1706223 (2018).
[39] G. Della Rosa, D. Vona, A. Aloisi, R. Ragni, R. Di Corato, M. Lo Presti, S. R. Cicco, E. Altamura, A. Taurino, M. Catalano, G. M. Farinola, and R. Rinaldi, *ACS Sust. Chem. & Eng.* **7**(2), 2207-2215 (2018).
[40] D. Vona, S. R. Cicco, R. Ragni, G. Leone, M. L. Presti, and G. M. Farinola, *MRS Comm.* **8**(3), 911-917 (2018).
[41] S. R. Cicco, D. Vona, E. De Giglio, S. Cometa, M. Mattioli- Belmonte, F. Palumbo, R. Ragni, and G. M. Farinola, *ChemPlusChem*, **80**(7), 1104-1112 (2015).
[42] S. R. Cicco, D. Vona, G. Leone, M. Lo Presti, F. Palumbo, E. Altamura, R. Ragni, and G. M. Farinola, *MRS Comm.* **7**(02), 214–220 (2017).
[43] A. Buccolieri, F. Italiano, A. Dell'Atti, G. Buccolieri, L. Giotta, A. Agostiano, F. Milano, and M. Trotta, *Annali di Chimica: J. Anal. Env. Cul. H. Chem.* **96**(3-4), 195-203 (2006).
[44] F. Mavelli, M. Trotta, F. Ciriaco, A. Agostiano, L. Giotta, F. Italiano, and F. Milano, *Eur. Biophys. J.* **43**, 301–315 (2014).
[45] G. Feher, *Photochem. and photobiol.* **14**(3), 373-387 (1971).
[46] S. C. Straley, W. W. Parson, D. C. Mauzerall, and R. K. Clayton, *Bioch. et Biophys. Act. (BBA)-Bioen.* **305**(3), 597-609 (1973).